



Journal of Advanced Research in Applied Mechanics

Journal homepage:
https://semarakilmu.com.my/journals/index.php/appl_mech/index
ISSN: 2289-7895



Development and Verification of a Half-body Railway Pantograph Model in the Vertical Directions

Munaliza Ibrahim¹, Mohd Azman Abdullah^{1,2*}, Mohd Hanif Harun^{1,2}, Fathiah Mohamed Jamil¹, Fauzi Ahmad^{1,2}, Ubaidillah Ubaidillah³

¹ Faculty of Mechanical Technology and Engineering, Universiti Teknikal Malaysia Melaka, Hang Tuah Jaya, 76100 Durian Tunggal, Melaka, Malaysia

² Centre for Advanced Research on Energy (CARE), Universiti Teknikal Malaysia Melaka, Hang Tuah Jaya, 76100 Durian Tunggal, Melaka, Malaysia

³ Mechanical Engineering Department, Universitas Sebelas Maret, Jl. Ir. Sutami 36A, Kentingan, Sukarta 57126, Indonesia

ARTICLE INFO

ABSTRACT

Article history:

Received 19 October 2023

Received in revised form 21 December 2023

Accepted 8 January 2024

Available online 23 February 2024

Keywords:

9DOF pantograph model; physics-based simulation; railway dynamic

In high-speed traffic, the pantograph-catenary system is responsible for the continuous supply of electrical power to the high-speed train. The pantograph-catenary system is stressed by the complex working environment in several ways. The excitation of the vehicle by the track is one of the normal disturbances of the pantograph-catenary interaction. In previous studies, only the vertical effect of vehicle-track vibration on pantograph-catenary interaction was considered. To address this deficiency, both pantograph-catenary and vehicle-track models are established in this work. The nine degrees of freedom (9DOF) of the railway pantograph model are analysed and verified by comparison with the 2D physics-based simulation software Algodo. The effects of weights, steps, and bumps are considered, and the responses of the mass contact strip are analysed. The same inputs are used in the MATLAB/Simulink model of the half-body railway pantograph. The results are compared for verification using an appropriate statistical analysis. It can be shown that the model is verified with a small percentage of deviations due to the actual gravity and spring deflections at different inputs. Statistical analysis for the mean absolute relative error is performed to capture the effects of random track irregularities on the pantograph-catenary interaction. The verification results show that the developed model can be used for vertical direction analysis and is also valuable and instructive for the future experimental approach of the active half-body railway pantograph.

1. Introduction

Railways are among the land transportation modes that are widely used in various countries to connect cities, transport goods, and provide public transportation services on certain routes [1,2]. The railway industry is working hard to perfect the design and technology to improve the safety, efficiency and comfort of rail transport. An electric train is usually powered by an engine or a locomotive, and the widely used system for continuous power transmission to the locomotive is the

* Corresponding author.

E-mail address: mohdazman@utem.edu.my

<https://doi.org/10.37934/aram.114.1.6682>

pantograph-catenary system [3], as shown in Figure 1 and Figure 2. The pantograph is usually installed on the roof of the train to connect with catenary wire, which is built along the track to provide a continuous power supply for an electric train. In general, the mechanical interaction between the pantograph and catenary is very important, because the quality of the current collection directly depends on the performance of the interaction between the pantograph and catenary, and stable sliding contact is a prerequisite for the quality of a good current collection [4]. This interaction is significant for ensuring a reliable current transmission without frequent loss of contact and excessive wear of the sliding surface [5]. The increasing speed of railways worldwide is creating significant engineering challenges including ride performances [6-8] and electrification through pantograph-catenary interaction [9], therefore, the study of pantograph-catenary interaction is gaining attention and popularity in both academia and industry.

Nowadays, there are many types of numerical pantograph-catenary models developed by many researchers around the world. Previous research has shown that pantographs are usually modeled by a two- or three-degree-of-freedom model, as this model provides an excellent approach for simulating the pantograph. The same is true for contact wires, which are usually modeled as a spring system with a lumped mass to describe the stiffness distribution along the long span. In 2019, Uehan gave a comprehensive overview of the railway-specific phenomena caused by the interaction of subsystems such as overhead lines, rolling stock, tracks, and structures to show the complex dynamic behavior of railroad systems [10]. Various disturbances are assumed to affect the performance of pantograph-catenary interaction, such as damage to railroad wheel treads [11], an irregularity in vertical track [12,13], the aerodynamic performance of collector strips [14], and irregular wear [15-17], which are considered in the numerical simulation. The findings from the above literature show that most researchers study the dynamic behavior of pantographs and overhead contact lines without considering disturbances in the vehicle trajectory. The interaction of the pantograph and the overhead contact line can be classified as vertical contact, and there is a probability that the vertical vibration of the vehicle has a significant effect on the contact of the pantograph and the overhead contact line. This is evidenced in a study by Song *et al.*, [18] by finding that the vertical vibrations of the car body have the greatest influence on the interaction between the pantograph and the overhead contact line. However, it is found that the dynamic behavior of the pantograph-catenary system is limited when disturbances between the vehicle and the track are considered.

In previous studies, pantograph-catenary models were validated by experiments with real models. Although the validation of the model using this method is accurate [19,20], the laboratory preparation for the actual pantograph-catenary model involves high testing costs and takes a long time [21]. These limitations have led numerical modelling to become the most popular approach [22] for studying the performance of pantograph-catenary interactions in academic circles and practical industries. Indeed, researchers often opt for numerical models [23,24] and verified pantograph catenary models with commercial software, since these models and simulations can be used and extended for more critical conditions to ensure the safe and reliable operation of electric trains without traffic disruptions [25]. Therefore, the main objective of the present work is to establish a half-body pantograph model for the vertical dynamic systems of railways.



Fig. 1. Simple overhead catenary



Fig. 2. Brecknell Willis TS-6034-type pantograph

Consequently, the primary objective of this research work is to develop a half-body railway pantograph model specifically designed for vertical directions. In this paper, the 9DOF lumped-mass model is adopted due to this model is an efficient approach for describing the physical characteristics of the real pantograph. The 9DOF railway pantograph model in MATLAB/Simulink is compared with a 2D physics-based simulation software, Algodoo. Algodoo is a freeware physics-based 2D sandbox from Algorix Simulation AB as a successor to a popular physics application known as Phun [26]. This software is always used as a learning tool, open computer game, animation tool and as an engineering tool [27]. Algodoo is also a very user-friendly software, aimed at real physics environment and visually attractive interface for motions and animations [28]. This software provides parameters such as mass, spring, and damper so that the motions and animations can be used to study the responses of the half-body railway pantograph to various inputs. However, to the best of the author's knowledge, no report has yet been found in which this software has been used to verify a half-body railway pantograph model specifically for vertical directions.

2. Methodology

2.1 Half-Body Railway Pantograph Modelling in MATLAB/Simulink

A schematic drawing of the half-body railway pantograph model is shown in Figure 3. This drawing describes the nine degrees of freedom (9 DOF) of the model, which consists of a 3DOF pantograph model with three moving masses and a 6 DOF car model that can move or bounce in the direction of uplift and pitch. The figure also defines the vehicle notation used in developing the model's equations of motion. All motions of the half-body railway pantograph are defined in a Newtonian reference frame moving at the constant forward speed of the vehicle.

The wheelsets are assumed to remain in constant contact with the rails. The suspension and mass distribution of the model are assumed to be symmetric so that the vertical and lateral dynamics of the model are decoupled. All flexibility is lumped into the suspension elements, which are modeled by linear springs and viscous dampers. The angular displacements are assumed to be small when the equations are linearized. The resulting equations of motion are given in Eq. (1) through Eq. (9) below. The derivation of these equations is straightforward and can be developed directly from Newton's laws of motion. The notation used in the equations is defined in Table 1.

The vertical dynamics model is intended to serve as a tool for evaluating the effects of variations in the design of the half-body railway pantograph suspension on the displacement and acceleration of the contact strip in response to track disturbances. The wheelset is excited by irregularities in the track profile. The model predicts the time history of the vertical of the pantograph contact strip. The system response variables important for evaluating the validity of the model of the vertical dynamics

of the half-body pantograph are the vertical and pitch accelerations of the car body, the vertical deflections of the primary wheelset and secondary suspension, the vertical and pitch accelerations of the bogies, the vertical of the pantograph frame, the vertical of the panhead, and the vertical of the contact strips. The accelerations of the contact strips are the primary outputs of the model, i.e., the outputs it is designed to predict.

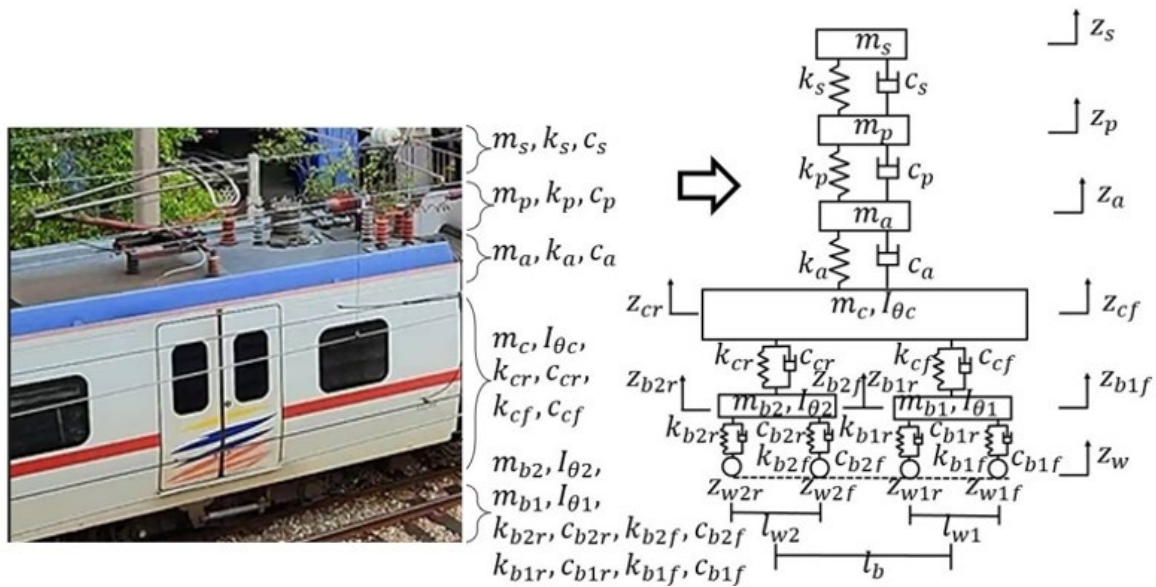


Fig. 3. Vertical dynamics model of the half-body railway pantograph

A half-body with nine degrees of freedom (9 DOF) of the railway pantograph system considered in this study developed by the vertical dynamic of the model, hence this research focuses on the performance of a railway pantograph model in vertical direction. A 3DOF pantograph model with three moving masses; contact strip, m_s , panhead, m_p , and frame, m_a which can move in the uplifts z_s, z_p, z_a respectively. 6 DOF car model with another three masses in motions; car body, m_c , which can move in the directions of uplift z_c and pitch θ_c directions. Two bogies, m_{b1} and m_{b2} that can bounce and pitch with $z_{b1f}, z_{b1r}, z_{b2f}, z_{b2r}$ respectively and four rigid wheelsets $Z_{w1f}, Z_{w1r}, Z_{w2f}, Z_{w2r}$. There are spring-damper elements $k_s, k_p, k_a, c_s, c_p, c_a$ between m_s and m_p , m_p and m_a , as well as between m_a and car body m_c . A secondary suspension system, consisting of a parallel configuration of spring and damper pairs $k_{cf}, k_{cr}, c_{cf}, c_{cr}$ is installed between the car body and bogie frame. The bogie frame, which includes two wheelsets, is connected to the wheelsets through a primary suspension system comprising pairs of springs $k_{b1r}, k_{b2r}, k_{b1f}, k_{b2f}$ and dampers $c_{b1r}, c_{b2r}, c_{b1f}, c_{b2f}$. For analysis purposes, the contact wire is modeled as a basic spring and damper system. All parameters should be defined based on the user experience in the numerical analysis. The larger the value of the spring and damper coefficient, the lower the numerical efficiency and the longer the running time, but the more accurate it is.

The equation of motion of this model is given by the equation of motion and pitch of the bogies and car body in Eq. (1) to Eq. (6), the equation of motion of the contact strip in Eq. (9), the equation of motion of the pan head in Eq. (8), and finally the equation of motion of the frame in Eq. (7). Consequently, all dynamic equilibrium equations of the half-body railway pantograph should be expressed as all equations below.

Table 1
 Notation for vertical half-body railway pantograph model

Symbol	Parameter	Units
Z_s	Vertical displacement of contact strip	m
Z_p	Vertical displacement of panhead	m
Z_a	Vertical displacement of frame	m
Z_{cf}	Vertical displacement of front car body	m
Z_{cr}	Vertical displacement of rear car body	m
Z_{b1f}	Vertical displacement of front bogie 1	m
Z_{b1r}	Vertical displacement of rear bogie 1	m
Z_{b2f}	Vertical displacement of front bogie 2	m
Z_{b2r}	Vertical displacement of rear bogie 2	m
Z_{w1f}	Vertical irregularity of front wheel 1	m
Z_{w1r}	Vertical irregularity of rear wheel 1	m
Z_{w2f}	Vertical irregularity of front wheel 2	m
Z_{w2r}	Vertical irregularity of rear wheel 2	m
$I_{\theta c}$	Pitch inertia of car body	kgm ²
$I_{\theta 1}$	Pitch angle of front bogie	kgm ²
$I_{\theta 2}$	Pitch angle of rear bogie	kgm ²
m_s	Mass of contact strip	kg
m_p	Mass of panhead	kg
m_a	Mass of frame	kg
m_c	Mass of car body	kg
m_{b1}	Mass of front bogie	kg
m_{b2}	Mass of rear bogie	kg
l_b	Distance between 2 bogies	m
l_{w1}	Distance between front wheels	m
l_{w2}	Distance between rear wheels	m
k_s	Vertical stiffness panhead to contact strip	Nm ⁻¹
k_p	Vertical stiffness arm to panhead	Nm ⁻¹
k_a	Vertical stiffness car body to frame	Nm ⁻¹
k_{cf}	Vertical stiffness front bogie to car body	Nm ⁻¹
k_{cr}	Vertical stiffness rear bogie to car body	Nm ⁻¹
k_{b1f}	Vertical stiffness wheel 1 to front bogie	Nm ⁻¹
k_{b1r}	Vertical stiffness wheel 1 to front bogie	Nm ⁻¹
k_{b2f}	Vertical stiffness wheel 2 to rear bogie	Nm ⁻¹
k_{b2r}	Vertical stiffness wheel 2 to rear bogie	Nm ⁻¹
c_s	Equivalent viscous damping panhead to contact strip	Nsm ⁻¹
c_p	Equivalent viscous damping frame to panhead	Nsm ⁻¹
c_a	Equivalent viscous damping car body to frame	Nsm ⁻¹
c_{cf}	Equivalent viscous damping front bogie to car body	Nsm ⁻¹
c_{cr}	Equivalent viscous damping rear bogie to car body	Nsm ⁻¹
c_{b1f}	Equivalent viscous damping wheel 1 to front bogie	Nsm ⁻¹
c_{b1r}	Equivalent viscous damping wheel 1 to front bogie	Nsm ⁻¹
c_{b2f}	Equivalent viscous damping wheel 2 to rear bogie	Nsm ⁻¹
c_{b2r}	Equivalent viscous damping wheel 2 to rear bogie	Nsm ⁻¹

$$m_{b1}\ddot{z}_{b1} = k_{b1r}(z_{w1r} - z_{b1r}) + c_{b1r}(\dot{z}_{w1r} - \dot{z}_{b1r}) + k_{b1f}(z_{w1f} - z_{b1f}) + c_{b1f}(\dot{z}_{w1f} - \dot{z}_{b1f}) - k_{cf}(z_{b1} - z_{cf}) - c_{cf}(\dot{z}_{b1} - \dot{z}_{cf}) \quad (1)$$

$$\ddot{\theta}_1 I_{b1} = \frac{l_{w1}}{2} [k_{b1f}(z_{w1f} - z_{b1f}) + c_{b1f}(\dot{z}_{w1f} - \dot{z}_{b1f})] - \frac{l_{w1}}{2} [k_{b1r}(z_{w1r} - z_{b1r}) + c_{b1r}(\dot{z}_{w1r} - \dot{z}_{b1r})] \quad (2)$$

$$m_{b2}\ddot{z}_{b2} = k_{b2r}(z_{w2r} - z_{b2r}) + c_{b2r}(\dot{z}_{w2r} - \dot{z}_{b2r}) + k_{b2f}(z_{w2f} - z_{b2f}) + c_{b2f}(\dot{z}_{w2f} - \dot{z}_{b2f}) - k_{cr}(z_{b2} - z_{cr}) - c_{cr}(\dot{z}_{b2} - \dot{z}_{cr}) \quad (3)$$

$$\ddot{\theta}_2 I_{b2} = \frac{l_{w2}}{2} [k_{b2f}(z_{w2f} - z_{b2f}) + c_{b2f}(\dot{z}_{w2f} - \dot{z}_{b2f})] - \frac{l_{w2}}{2} [k_{b2r}(z_{w2r} - z_{b2r}) + c_{b2r}(\dot{z}_{w2r} - \dot{z}_{b2r})] \quad (4)$$

$$\ddot{z}_c m_c = k_{cr}(z_{b2} - z_{cr}) + c_{cr}(\dot{z}_{b2} - \dot{z}_{cr}) + k_{cf}(z_{b1} - z_{cf}) + c_{cf}(\dot{z}_{b1} - \dot{z}_{cf}) - k_a(z_c - z_a) - c_a(\dot{z}_c - \dot{z}_a) \quad (5)$$

$$\ddot{\theta}_c I_c = \frac{l_b}{2} (k_{cf}(z_{b1} - z_{cf}) + c_{cf}(\dot{z}_{b1} - \dot{z}_{cf})) - \frac{l_b}{2} (k_{cr}(z_{b2} - z_{cr}) + c_{cr}(\dot{z}_{b2} - \dot{z}_{cr})) \quad (6)$$

$$\ddot{z}_a m_a = k_a(z_c - z_a) + c_a(\dot{z}_c - \dot{z}_a) - k_p(z_a - z_p) - c_p(\dot{z}_a - \dot{z}_p) \quad (7)$$

$$\ddot{z}_p m_p = k_p(z_a - z_p) + c_p(\dot{z}_a - \dot{z}_p) - k_s(z_p - z_s) - c_s(\dot{z}_p - \dot{z}_s) \quad (8)$$

$$\ddot{z}_s m_s = k_s(z_p - z_s) + c_s(\dot{z}_p - \dot{z}_s) \quad (9)$$

2.2 Half-Body Railway Pantograph Modelling in Algodoo

In this study, the half-body railway pantograph model is simplified to 9DOF lumped model with six masses in motions; contact strip, pan head, frame, car body, bogies and wheelsets as seen in Figure 4 which can characterize the vertical motion of the half-body railway pantograph effectively. While the component of catenary wire is depicted by a simple spring and damper for analysis. Initially, only the weights of the masses affect the motions as depicted in Figure 4(a) show the responses at z_s while as Figure 4(b) show the responses at z_{w1f} .

In the second simulation, step input (z_{w1f}) of 0.125 m (Figure 5b) is applied. Thirdly, a bumper input (z_{w1f}) of 0.1875 m (Figure 5a) is applied. Due to the software constraint to produce such inputs, the bottom support of the pantograph is modified to a rotational part (Figure 5). The inputs are assumed directly from track to body to the pantograph support. The input is move and hit the support at certain force. In general, the linearization of the frame's nonlinear motion equation at a specific height can be used to determine the lumped mass of the frame. Considering this, a simplified linear model of the half-body railway pantograph is produced, which comprises of the damper and the spring as it mass. This model can accurately define the half-body railway pantograph's vertical motion by considering the masses' weights only.

This study used a combination of MATLAB/Simulink based on the zero-dimensional model to build the railway pantograph model according to the mathematical equations above. The model should include the input z_{w1f} from Algodoo as the disturbance to generate the output of vertical displacement z_s . The damping ratio is expressed as:

$$\xi = \frac{c}{2\sqrt{km}} \tag{10}$$

where ξ is the damping ratio, c is the equivalent viscous damping, k is the vertical stiffness and m is the mass of each element.

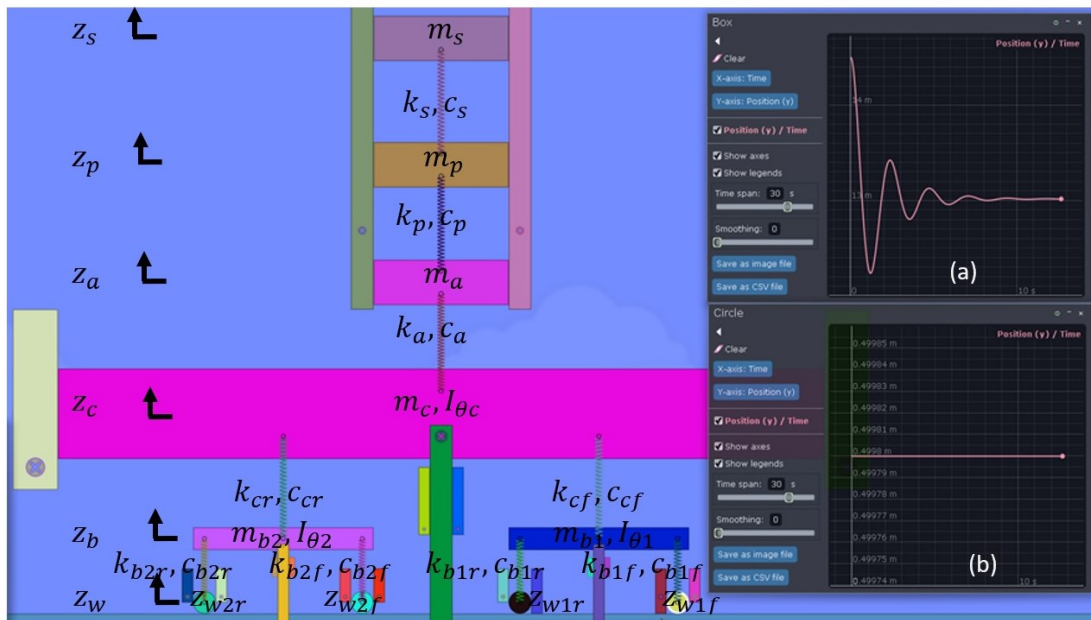


Fig. 4. Half-body simulation in Algodoo (a) Responses at z_s (b) Responses at z_{w1f}

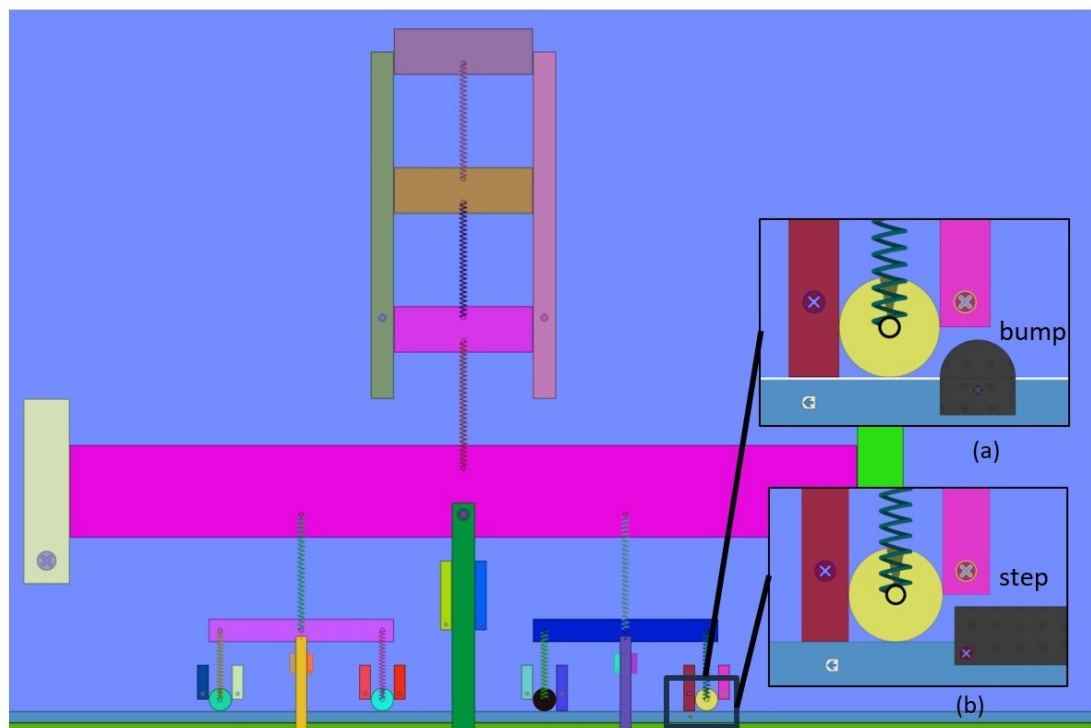


Fig. 5. Simulation inputs (a) bump input (b) step input

2.3 Damping and Stiffness Parametric Analysis

The data for some of the structural stiffnesses and damping are nonlinear. Since the model is linear, a procedure had to be used to linearize this data. This procedure could be applied iteratively to correct the values for each input. The sensitivity of the predicted responses to errors in the parameters could be calculated using parametric analysis of the damping and stiffness. Statistical errors used in analysis to evaluate the accuracy or error of the model include the mean absolute relative error and its percentage. Statistical error is an element of uncertainty in statistics that can occur when a sample of data is used to make statistical estimates or inferences about a larger population. Mean absolute relative error measures the average absolute value of the relative error between the predicted values and the actual value in a data set, while mean absolute percentage error measures the average absolute value of the relative error percentage between the predicted values and the actual value in a data set. The error from the both models (ε_i) can be calculated by using Eq. (11), the mean absolute relative error ($\bar{\varepsilon}$) can be calculated by using Eq. (12) while the mean absolute percentage error ($\% \bar{\varepsilon}$) formula is represented in Eq. (13). Table 2 shows the range of damping ratio used in order to find the optimal damping ratio at the lowest error in the half-body railway pantograph model.

$$\varepsilon_i = |x_{A,i} - x_{M,i}| \quad (11)$$

$$\bar{\varepsilon} = \frac{\sum_{i=1}^n \left| \frac{x_{A,i} - x_{M,i}}{x_{A,i}} \right|}{n} \quad (12)$$

$$\% \bar{\varepsilon} = \frac{\sum_{i=1}^n \left| \frac{x_{A,i} - x_{M,i}}{x_{A,i}} \right|}{n} \times 100 \quad (13)$$

where ε_i refers to error values between Algodo model $x_{A,i}$ and MATLAB/Simulink model $x_{M,i}$ while as $\bar{\varepsilon}$ is the mean absolute relative error, $\% \bar{\varepsilon}$ is the mean absolute percentage error and n is the total set of data used in the simulation. The parametric analysis of damping is initiated by changing the value of the damping ratio, which includes the value of c_{b1f} and c_{b1r} . If the value of the damping ratio is changed gradually, no optimal value is obtained. Therefore, the analysis must be performed by first changing both damping ratios for m_{b1} , followed by changes in m_{b2} .

This procedure yields the optimal value for the damping ratio with the least error, as shown in Figure 6 and Figure 7. The effect of different damping ratio parameters for each mass was investigated. Simulated system performance was evaluated for the damping ratio values listed in Table 2. Basically, the tuning range is between 0 and 2 in agreement with the lowest error presented. Consequently, from the obtained optimal value for the damping ratio, the damping coefficient can be derived by the above Eq. (10). The information from this table shows that at this stage of the parametric analysis, the lowest error is 0.0221. As seen from Figure 8 to Figure 12 the damping parametric analysis for required damping coefficient are obtained.

Next, the parametric analysis of stiffness is performed to find the least error. The analysis is performed only for both bogies since the error value obtained when the stiffness value is changed at

other locations will give a higher error value. As shown in Figures 13 and 14, the parametric analysis of stiffness is performed for the required stiffness. Once the parameter variables of the optimum stiffness are determined, the responses of the half-body railway pantograph system can be calculated. The simulated system performance was evaluated for the stiffness ratios listed in Table 3. From this table, the optimal value of the mean absolute relative error resulting from the parametric analysis of the stiffness is 0.0173, where the mean absolute percentage error is 1.73%.

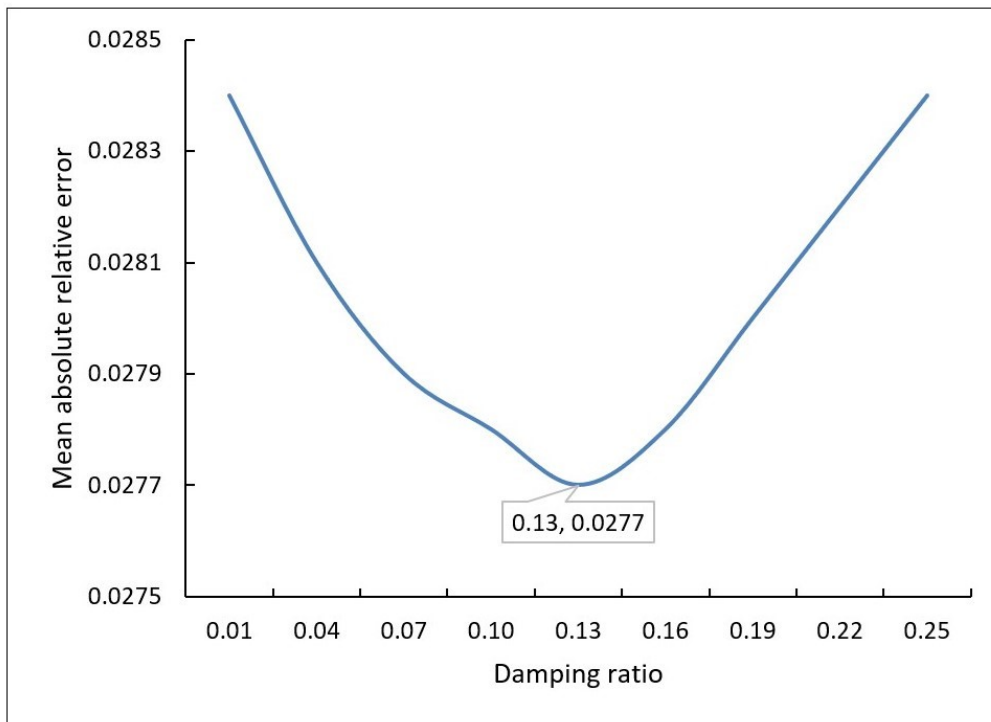


Fig. 6. Damping parametric analysis for c_{b1f} and c_{b1r}

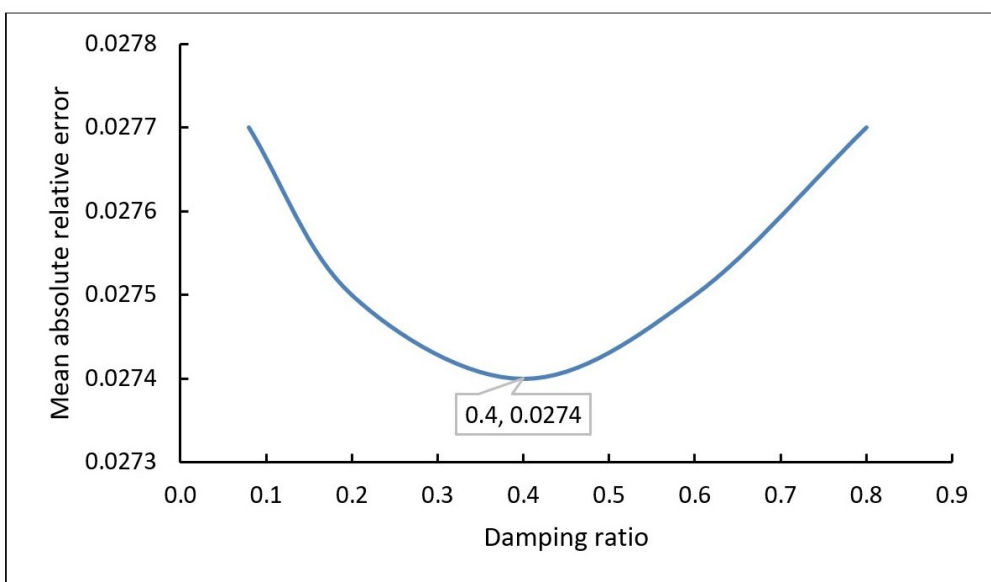


Fig. 7. Damping parametric analysis for c_{b2f} and c_{b2r}

Table 2
 Damping parametric analysis value

Parameter	Tunning range	Optimal value	Mean absolute relative error	Damping Coefficient
c_{b1f}, c_{b1r}	0 - 0.3	0.13	0.0277	11.2051
c_{b2f}, c_{b2r}	0 - 1.0	0.40	0.0274	34.4771
c_{cr}	0 - 1.0	0.45	0.0254	73.9425
c_{cf}	0 - 2.0	0.65	0.0224	106.8059
c_a	0 - 1.0	0.60	0.0222	50.9117
c_p	0 - 1.0	0.70	0.0221	59.3970
c_s	0 - 2.0	0.95	0.0221	80.6102

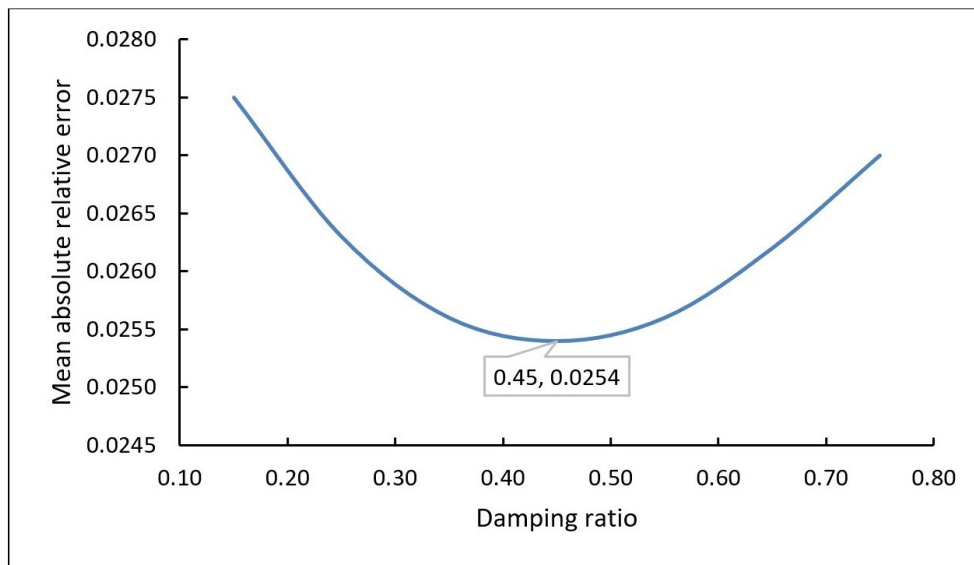


Fig. 8. Damping parametric analysis for c_{cr}

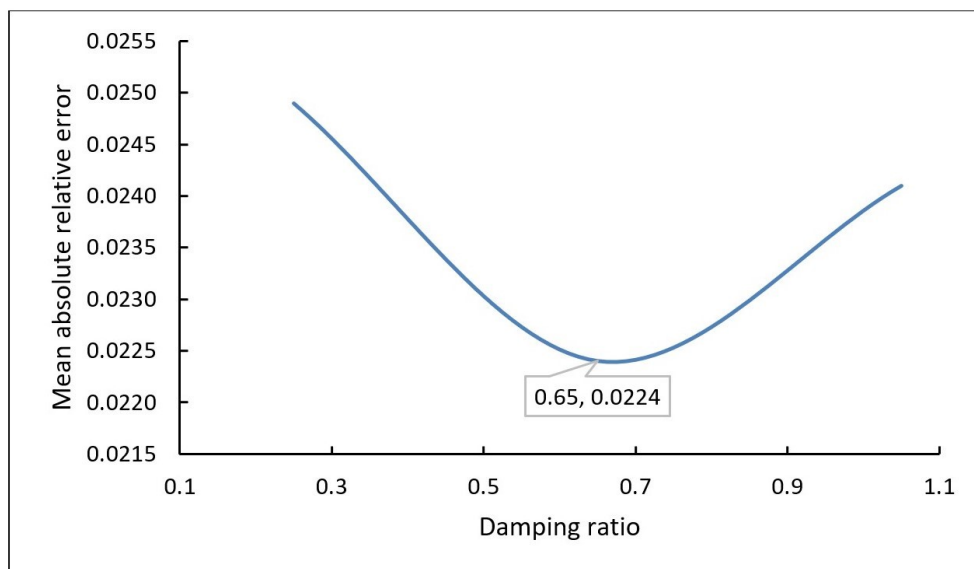


Fig. 9. Damping parametric analysis for c_{cf}

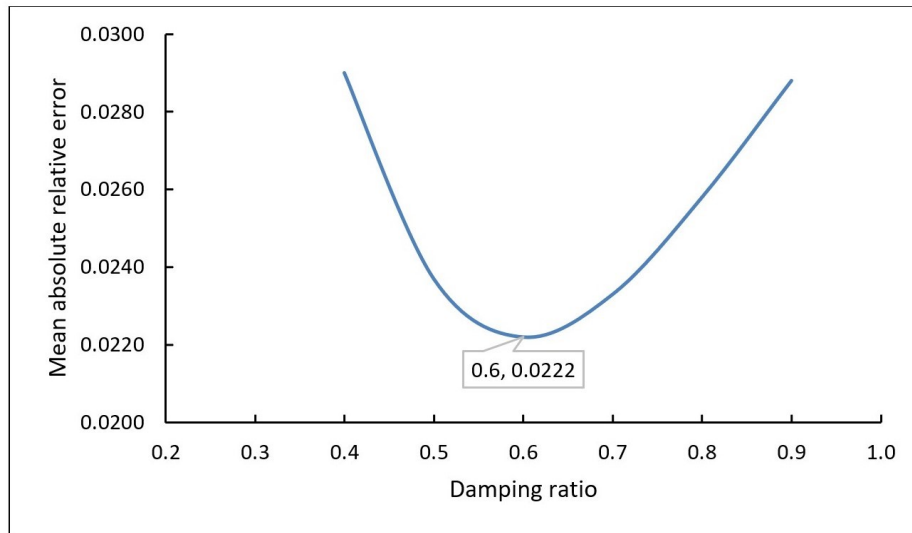


Fig. 10. Damping parametric analysis for c_a

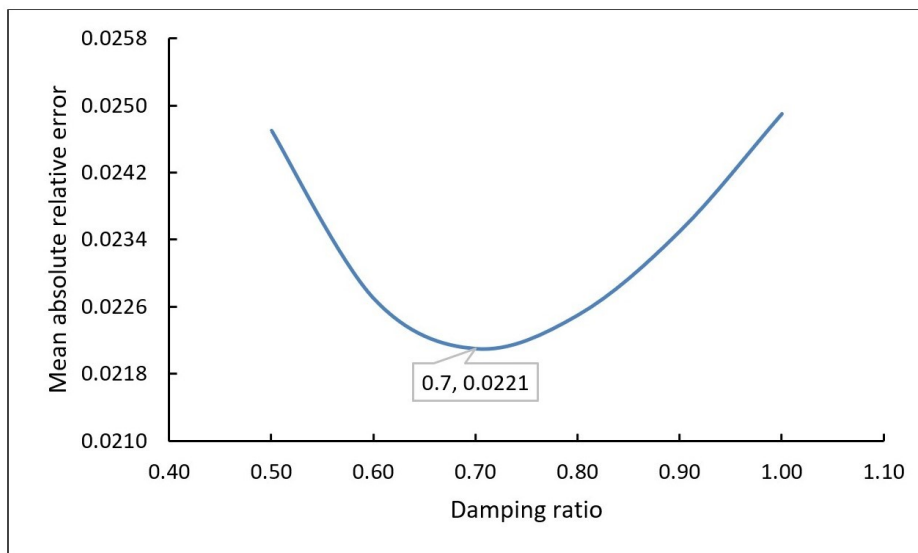


Fig. 11. Damping parametric analysis for c_p

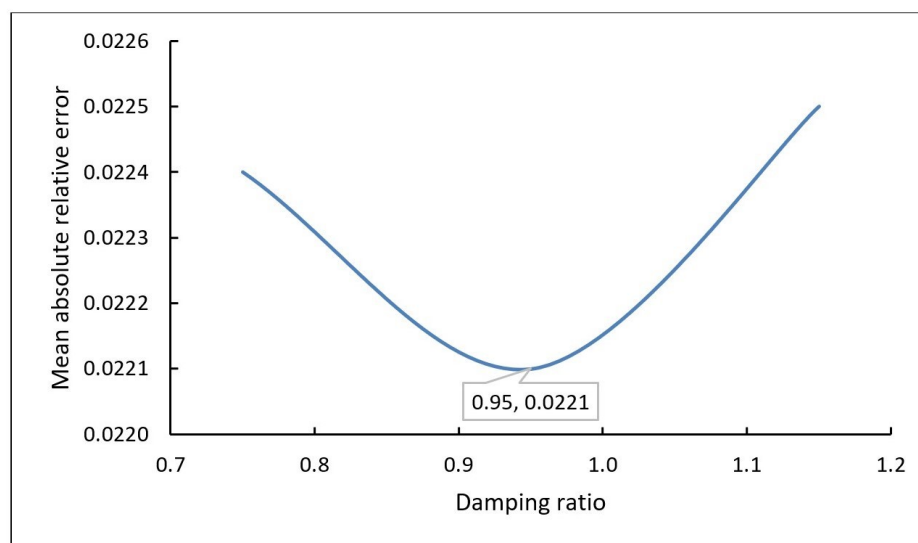


Fig. 12. Damping parametric analysis for c_s

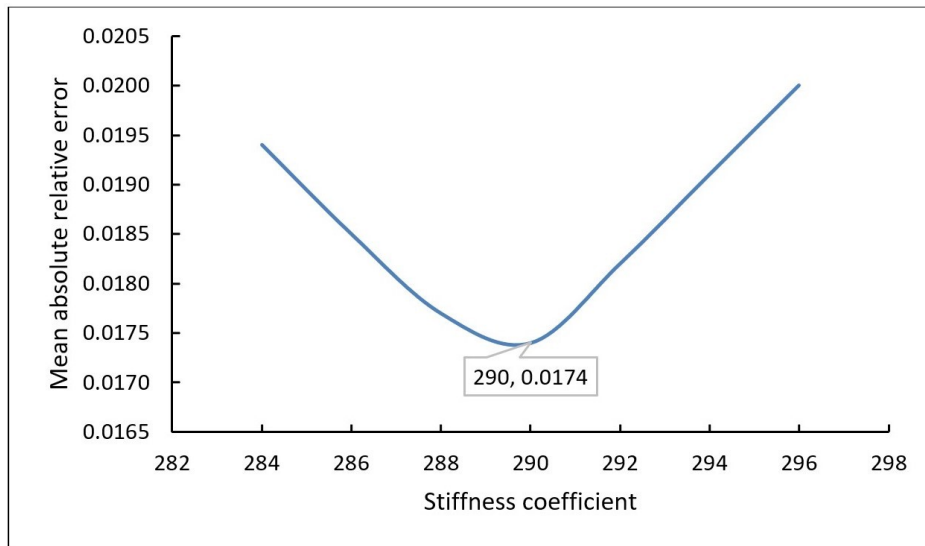


Fig. 13. Stiffness parametric analysis for k_{b1f} and k_{b1r}

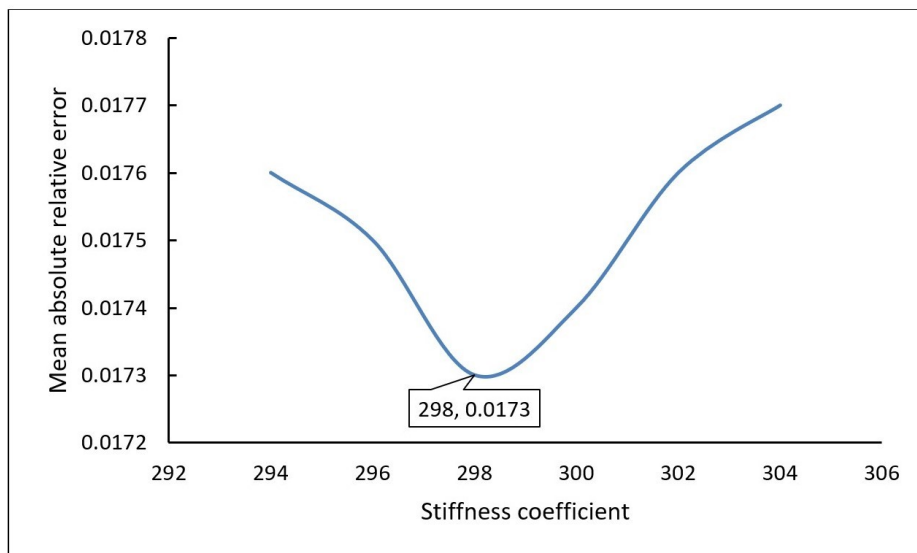


Fig. 14. Stiffness parametric analysis for k_{b2f} and k_{b2r}

Table 3

Stiffness parametric analysis value

Parameter	Tunning range	Optimal value	Mean absolute relative error
k_{b1f}, k_{b1r}	280 - 300	290	0.0174
k_{b2f}, k_{b2r}	300 - 310	298	0.0173

3. Results and Discussion

In this study, three different values of input such as weight, step and bump were selected for the simulation test represent the track irregularities was given to the system at front wheel z_{w1f} . The initial state of a system greatly affects the dynamic results of the simulation. Before the system runs at a certain speed, the action of tension and gravity leads to an initial disturbance of the system to reach an initial state of equilibrium. Therefore, the correct initial equilibrium conditions must be calculated and supplied to this model to obtain an accurate dynamic response. Verification procedure

is initiated with the analysis responses of contact strip displacement z_s at masses motion then followed by step input at 0.125 m and finally bump input at 0.1875 m. Each of the results are analysed in term of the mean absolute relative error for both simulation and Algodoo data and measure the percentage of errors. The Algodoo model is plotted blue solid line while the Simulink model is plotted with red dashed line. It can be observed that the responses are almost the same between the Simulink model and the Algodoo model. The differences are due to the damping parameters; the damping ratio is used in the Algodoo, while the actual damping value is used in MATLAB/Simulink which is depending on the mass and spring stiffness. The mean absolute relative error between the models is depicted in Table 3 for no input (weight only), step input, and bump input respectively. The mean absolute percentage error is less than 2.5 % compared to the results in Algodoo.

3.1 Weight Input

Figure 15 depicts the responses of contact strip displacement z_s at masses motion. It can be seen that due to the influence of tension and gravity, the minimum time to reach initial equilibrium should be greater than 10 s. It can be observed that the responses are almost the same between the Simulink model and the Algodoo model with the mean relative absolute error between the models is 0.0173.

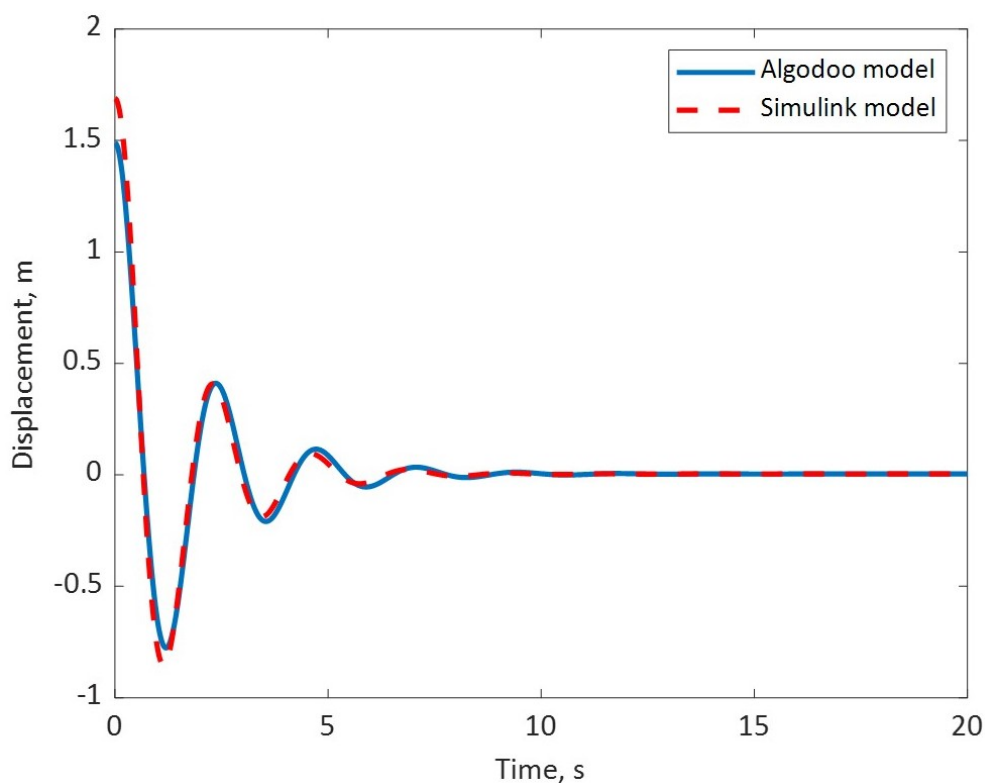


Fig. 15. Vertical displacement output responses of contact strip for weight considering only

3.2 Step Input

Figure 16 below show the vertical displacement at z_s when disturb by the step input. Numerical simulations show that the application of the input is given after the system reach the initial equilibrium at 11 s. Figure shows that the displacement time series obtained from the numerical model describes the real response well, including both displacement magnitude during the whole

passage and the shape with the mean relative absolute error between the models is 0.022. There is a peak in the figure when the system is disturbed by the input.

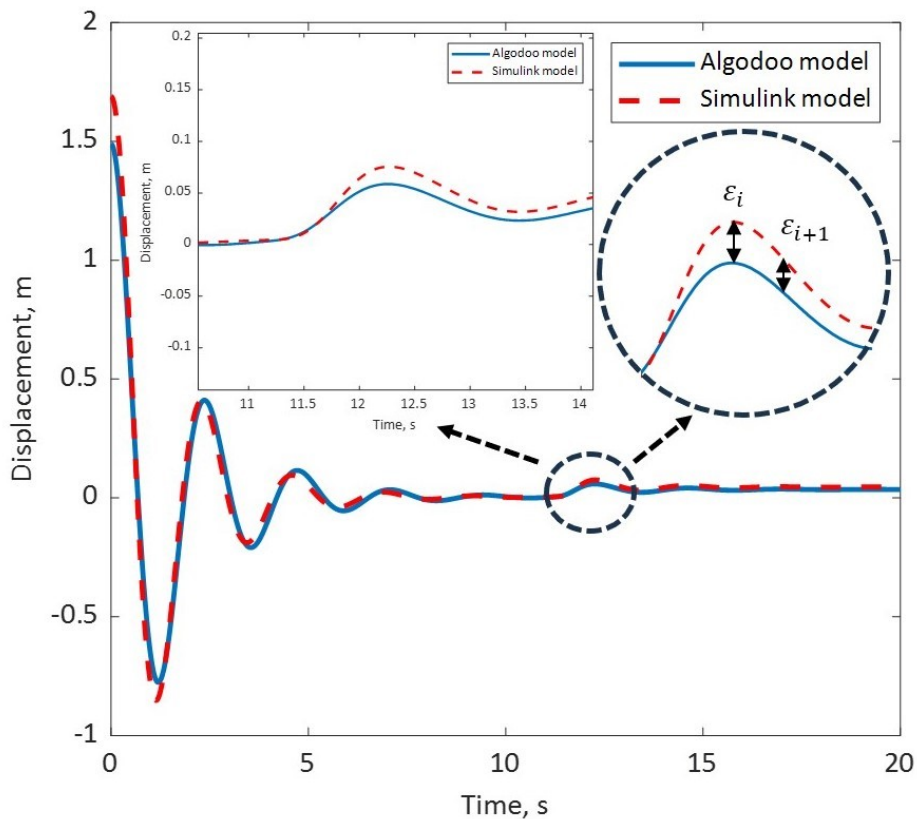


Fig. 16. Vertical displacement output responses of contact strip for step input

3.3 Bump Input

Figure 17 below show the vertical displacement at z_s when disturb by the bump input after the system reach the initial equilibrium at 13 s. It can be observed that due to the effect of input, the fluctuation in displacement value is significantly increased, manifested by the increase of minimum value and the decrease of maximum value. The mean relative absolute error between the models is 0.023.

3.4 Mean Absolute Relative Error Analysis

The results for mean absolute relative error and mean absolute percentage error under different input are presented in Table 4. Noted that the lower the error value, the better the accuracy of the model because, the error analysis measures the relative error in the form of a percentage against the range of true values. It gives an idea of how closely the model or prediction approaches the variation of the true values in the dataset.

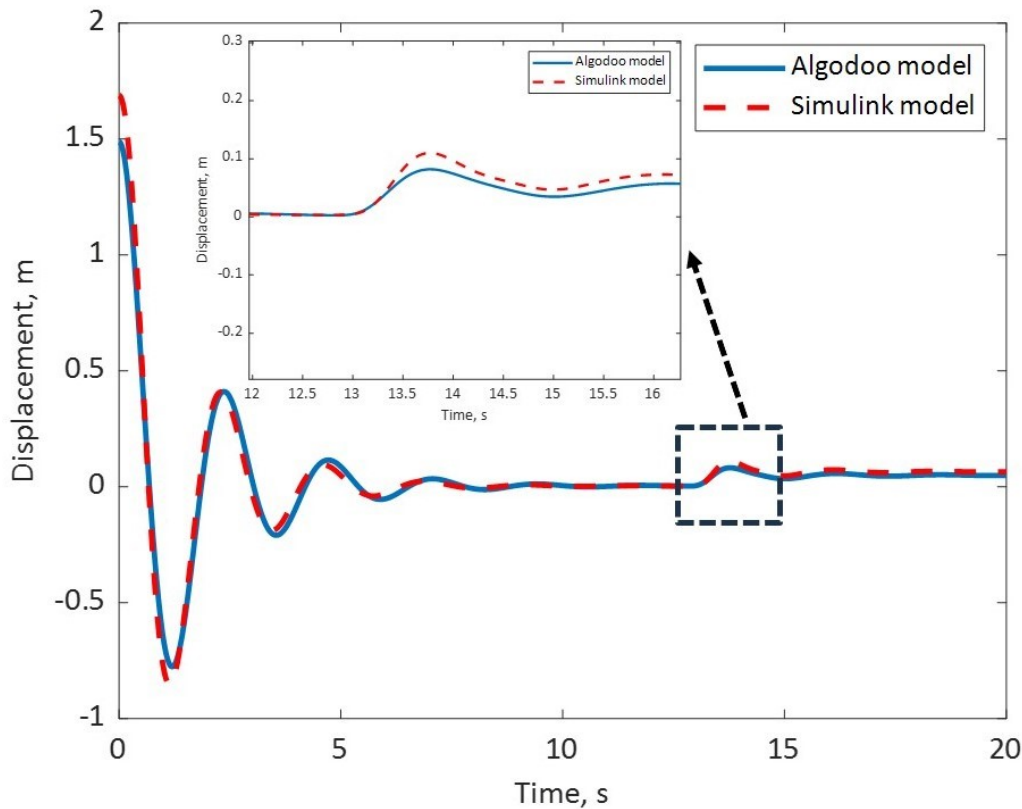


Fig. 17. Vertical displacement output responses of contact strip for bump input

Table 4
 Statistics of error in different inputs

Input	Mean Absolute Relative Error before tuning	Mean Absolute Relative Error after tuning
Weight	3.4996×10^{-2}	1.7340×10^{-2}
Step	3.9063×10^{-2}	2.1613×10^{-2}
Bump	3.9762×10^{-2}	2.2543×10^{-2}

4. Conclusions

The 9DOF model with the lumped mass is used to describe the physical characteristics of the real pantograph. The results show a good and clear explanation of the vertical displacement of the contact strip of the real pantograph in terms of the mean absolute relative error for both the Algodo simulation and the MATLAB/Simulink model. The simulations were performed with the model of a half-body railway pantograph using different input weights, steps, and bumps. Since the differences are very small, which are less than 2.5 %, it can be concluded that the models are verified. The results of the verification show satisfactory performance of the developed model in MATLAB/Simulink compared with a 2D physics-based simulation software, Algodo model with acceptable error. Both models can be used for further analysis of the interaction between pantographs and overhead contact lines to obtain results from experimental measurements.

Acknowledgement

The authors gratefully acknowledge the funded received form this research from the Centre for Advanced Research on Energy (CARE) and the Universiti Teknikal Malaysia Melaka, Malacca, Malaysia

under grant: PJP/2023/CARE/EV/Y00012. The authors also gratefully acknowledge the support and collaboration from Universitas Sebelas Maret, Sukarta, Indonesia.

References

- [1] Juhari, Mohammad Lui, and Kadir Arifin. "Validating measurement structure of materials and equipment factors model in the MRT construction industry using confirmatory factor analysis." *Safety Science* 131 (2020): 104905. <https://doi.org/10.1016/j.ssci.2020.104905>.
- [2] AbdelGawad, Ahmed Farouk, Naser Mohammed Aljameel, and Ramy Elsayed Shaltout. "Computational Modelling of the Aerodynamic Noise of the Full-Scale Pantograph of High-Speed Trains." *Journal of Advanced Research in Fluid Mechanics and Thermal Sciences* 93, no. 1 (2022): 94-109. <https://doi.org/10.37934/arfmts.93.1.94109>.
- [3] Parlakyildiz, Şakır, Muhsin Gençoğlu, and Mehmet Sait Cengiz. "Electric Train Application Study For Catenary-Pantograph Interaction." *Avrupa Bilim ve Teknoloji Dergisi* 20 (2020): 506-515. <https://doi.org/10.31590/ejosat.759407>.
- [4] Wang, Zhiyong, Qi Zhou, Fengyi Guo, Aixia Tang, Xili Wang, and Xi Chen. "Mathematical model of contact resistance in pantograph-catenary system considering rough surface characteristics." *IEEE Transactions on Transportation Electrification* 8, no. 1 (2021): 455-465. <https://doi.org/10.1109/TTE.2021.3095120>.
- [5] Shi, Haijian, Guo Chen, and Yiren Yang. "A comparative study on pantograph-catenary models and effect of parameters on pantograph-catenary dynamics under crosswind." *Journal of Wind Engineering and Industrial Aerodynamics* 211 (2021): 104587. <https://doi.org/10.1016/j.jweia.2021.104587>.
- [6] Ibrahim, Munaliza, Mohd Azman Abdullah, Fathiah Mohamed Jamil, Mohd Hanif Harun, and Fauzi Ahmad, "Ride Index Performances of High-Speed Railway Trains." *Journal of Engineering and Technology* 14, no. 2 (2023): 1-15. <https://jet.utem.edu.my/jet/article/download/6368/4253>.
- [7] Mohamed Jamil, Fathiah, Mohd Azman Abdullah, Mohd Hanif Harun, Munaliza Ibrahim, Fauzi Ahmad, and Ubaidillah Ubaidillah, "Analysis of Active Secondary Suspension with Modified Skyhook Controller to Improve Ride Performance of Railway Vehicle." *Jurnal Teknologi* 85, no. 5 (2023): 43-54. <http://dx.doi.org/10.11113/jurnalteknologi.v85.19771>.
- [8] Mohamed Jamil, Fathiah, Mohd Hanif Harun, Mohd Azman Abdullah, Munaliza Ibrahim, and Fauzi Ahmad. "Railway car body lateral hunting attenuation using body-based modified skyhook control for secondary suspension." *Proceedings of Mechanical Engineering Research Day 2022* (2022): 234-235. https://www3.utem.edu.my/care/proceedings/merd22/pdf/09%20Structural%20and%20Mechanical%20Testing/110_p234_235.pdf.
- [9] Ibrahim, Munaliza, Mohd Azman Abdullah, Mohd Hanif Harun, Fathiah Mohamed Jamil, and Fauzi Ahmad. "Railway Pantograph Model Verification and Analysis." *Proceedings of Mechanical Engineering Research Day 2022* (2022): 107-108.
- [10] Uehan, Fumiaki. "Recent Research and Development in Railway Dynamics." *Quarterly Report of RTRI* 60, no. 1 (2019): 10-13. https://doi.org/10.2219/rtrigr.60.1_10.
- [11] Maglio, Michele, Tore Vernersson, Jens CO Nielsen, Anders Ekberg, and Elena Kabo. "Influence of railway wheel tread damage on wheel-rail impact loads and the durability of wheelsets." *Railway Engineering Science* (2023): 1-16. <https://doi.org/10.1007/s40534-023-00316-2>.
- [12] Nasrollahi, Kourosh, Jens CO Nielsen, Emil Aggestam, Jelke Dijkstra, and Magnus Ekh. "Prediction of long-term differential track settlement in a transition zone using an iterative approach." *Engineering Structures* 283 (2023): 115830. <https://doi.org/10.1016/j.engstruct.2023.115830>.
- [13] Xu, Lei, and Wanming Zhai. "A model for vehicle-track random interactions on effects of crosswinds and track irregularities." *Vehicle system dynamics* 57, no. 3 (2019): 444-469. <https://doi.org/10.1080/00423114.2018.1469775>.
- [14] Dai, Zhi-yuan, Tian Li, Wei-hua Zhang, and Jiye Zhang. "Numerical study on aerodynamic performance of high-speed pantograph with double strips." *Fluid Dyn Mater Process* 16, no. 1 (2020): 31-40. <https://doi.org/10.32604/fdmp.2020.07661>.
- [15] Na, Kyung-Min, Kiwon Lee, and Hyungchul Kim. "Condition Monitoring of Railway Pantograph Using R-CNN and Image Processing." *Journal of Electrical Engineering & Technology* 18, no. 3 (2023): 2407-2416. <https://doi.org/10.1007/s42835-022-01229-6>.
- [16] N. Zhou, Y. Cheng, X. Zhang, X. Zhi, and W. Zhang, "Wear rate and profile prediction of Cu-impregnated carbon strip for high-speed pantograph," *Wear*, vol. 530, p. 205056, 2023, doi: <https://doi.org/10.1016/j.wear.2023.205056>.
- [17] Zhou, Ning, Yao Cheng, Xing Zhang, Xingshuai Zhi, and Weihua Zhang. "Wear rate and profile prediction of Cu-impregnated carbon strip for high-speed pantograph." *Wear* 530 (2023): 205056. <https://doi.org/10.1016/j.wear.2023.205056>

- [18] Song, Yang, Zhiwei Wang, Zhigang Liu, and Ruichen Wang. "A spatial coupling model to study dynamic performance of pantograph-catenary with vehicle-track excitation." *Mechanical Systems and Signal Processing* 151 (2021): 107336. <https://doi.org/10.1016/j.ymssp.2020.107336>.
- [19] Mohammad, Nur Syaza Syahira, Ili Shairah Abdul Halim, Siti Lailatul Mohd Hassan, and Wan Fazlida Hanim Abdullah. "Design and Performance Analysis of Sound Source Localization using Time Difference of Arrival Estimation." *Journal of Advanced Research in Applied Mechanics* 106, no. 1 (2023): 14-26. <https://doi.org/10.37934/aram.106.1.1426>.
- [20] Rahmat, Muhammad Syakirin, Shahrul Niza Mokhatar, Barizah Atirah Razali, Josef Hadipraman, and Seyed Jamalaldin Seyed Hakim. "Numerical Modelling of Impact Loads on RC Beams Utilizing Spent Garnet as a Replacement for Fine Aggregate." *Journal of Advanced Research in Applied Mechanics* 107, no. 1 (2023): 41-54. <https://doi.org/10.37934/aram.107.1.4154>.
- [21] Yang, Jia, Yang Song, Xiaobing Lu, Fuchuan Duan, Zhigang Liu, and Ke Chen. "Validation and analysis on numerical response of super-high-speed railway pantograph-catenary interaction based on experimental test." *Shock and Vibration* 2021 (2021): 1-13. <https://doi.org/10.1155/2021/9922404>.
- [22] Abidin, Mohamad Naufal Zainal, and Md Yushalify Misro. "Numerical Simulation of Heat Transfer using Finite Element Method." *Journal of Advanced Research in Fluid Mechanics and Thermal Sciences* 92, no. 2 (2022): 104-115. <https://doi.org/10.37934/arfmts.92.2.104115>.
- [23] Crasta, Asha, Khizer Ahmed Pathan, and Sher Afghan Khan. "Numerical simulation of surface pressure of a wedge at supersonic Mach numbers and application of design of experiments." *Journal of advanced research in applied mechanics* 101, no. 1 (2023): 1-18. <https://doi.org/10.37934/aram.101.1.118>.
- [24] Zakaria, Nur Nadia Mohd, Rohaida Che Man, Siti Zubaidah Sulaiman, Siti Kholijah Abdul Mudalip, Nor Hasmaliana Abdul Manas, and Laura Navika Yamani. "Optimization of Process Parameters of Immobilized Escherichia Coli for Cyclodextrin Production." *Journal of Advanced Research in Applied Mechanics* 107, no. 1 (2023): 1-10. <https://doi.org/10.37934/aram.107.1.110>.
- [25] Soodmand, Iman, Kourosh Heidari Shirazi, and Shapour Moradi. "Analysis of ride comfort of a continuous tracked bogie system with variable configuration." *Proceedings of the Institution of Mechanical Engineers, Part D: Journal of Automobile Engineering* 234, no. 14 (2020): 3429-3439. <https://doi.org/10.1177/0954407020931684>.
- [26] da Silva, Samir L., Rodrigo L. da Silva, Judismar T. Guaitolini Junior, Elias Gonçalves, Emilson R. Viana, and João BL Wyatt. "Animation with Algodoo: A simple tool for teaching and learning physics." *arXiv preprint arXiv:1409.1621* (2014). <https://doi.org/10.48550/arXiv.1409.1621>.
- [27] Gregorcic, Bor, and Madelen Bodin. "Algodoo: A tool for encouraging creativity in physics teaching and learning." *The Physics Teacher* 55, no. 1 (2017): 25-28. <https://doi.org/10.1119/1.4972493>.
- [28] Euler, Elias, Christopher Prytz, and Bor Gregorcic. "Never far from shore: productive patterns in physics students' use of the digital learning environment Algodoo." *Physics Education* 55, no. 4 (2020): 045015. <https://doi.org/10.1088/1361-6552/ab83e7>.